SUPPORTING INFORMATION

Single-cell Mass Spectrometry Reveals Small Molecules that Affect Cell Fates in the 16-cell Embryo

Rosemary M. Onjiko[a], Sally A. Moody[b], and Peter Nemes[a,1]

[a]Department of Chemistry, W. M. Keck Institute for Proteomics Technology and Applications, The George Washington University, 800 22nd Street, NW, Suite 4000, Washington, DC 20052, USA; [b]Department of Anatomy and Regenerative Biology, School of Medicine and Health Sciences, The George Washington University, 2300 I Street, NW, Washington, DC 20037, USA

[1]Correspondence to: Peter Nemes, Department of Chemistry, The George Washington University, 800 22nd Street, NW, Suite 4000, Washington, DC 20052, USA, (Tel) 1-202-994-5663, petern@gwu.edu

DETECTION LIMIT AND QUANTITATION

The analytical performance of our custom-built CE-μESI-MS platform was thoroughly characterized for identification and quantitation. The lower limit of detection and linear dynamic concentration range of quantitation were determined for chemical standards, and the quantitative reproducibility (relative % error) of both separation time and electropherographic peak area were determined for a given blastomere that was measured in multiple technical replicates.

The **lower limit of detection** was calculated as the concentration of analyte that yielded a signal-to-noise ratio (S/N) of 3, where S/N was defined as the peak height-to-noise root mean square ratio, as also shown in **Figure S1A**. The lower limit of detection was <10 nM (60 amol) for acetylcholine, and comparable figures were obtained for several other small molecules, including methionine and histidine. Slightly higher lower limit of detection applied to threonine (**Fig. S1A**). These limits of detection were sufficient to measure endogenous metabolite concentrations, which have independently been found to range from 100 μM to 2 mM in the whole embryo (1). The instrument provided **quantitative** response between the ~10 nM-to-1 μM tested range for these small molecules (see **Fig. S1A**). The digitizer of the mass spectrometer that was used in this study, an Impact HD (Bruker), is expected to extend this quantitative range to 4–5-orders of magnitude.

Endogenous metabolite amounts were quantified in $V11_{6–8}$ and $D11_{6–8}$ blastomeres with a 90-nL average volume in the 16-cell embryo using external calibration curves for standard metabolites. Despite the inherent chemical complexity of metabolites, the mean **reproducibility** was 5.7% in migration time and 22.3% in peak area for 10 technical replicates for a given blastomere (the $V11_1$) that was repeatedly measured over 4 consecutive days, as shown in **Figure S1B**. Hence, quantitation was sufficiently reproducible to decipher differential activities for various endogenous metabolites. A fold change ≥ 2.0 indicated biological significance, and statistical significance was marked at $p < 0.05$ using a two-tailed Student's t-test. These results demonstrate that the CE-ESI-MS platform accomplished robust and reproducible operation throughout the course of this study, allowing us to query small-molecule differences between blastomeres.

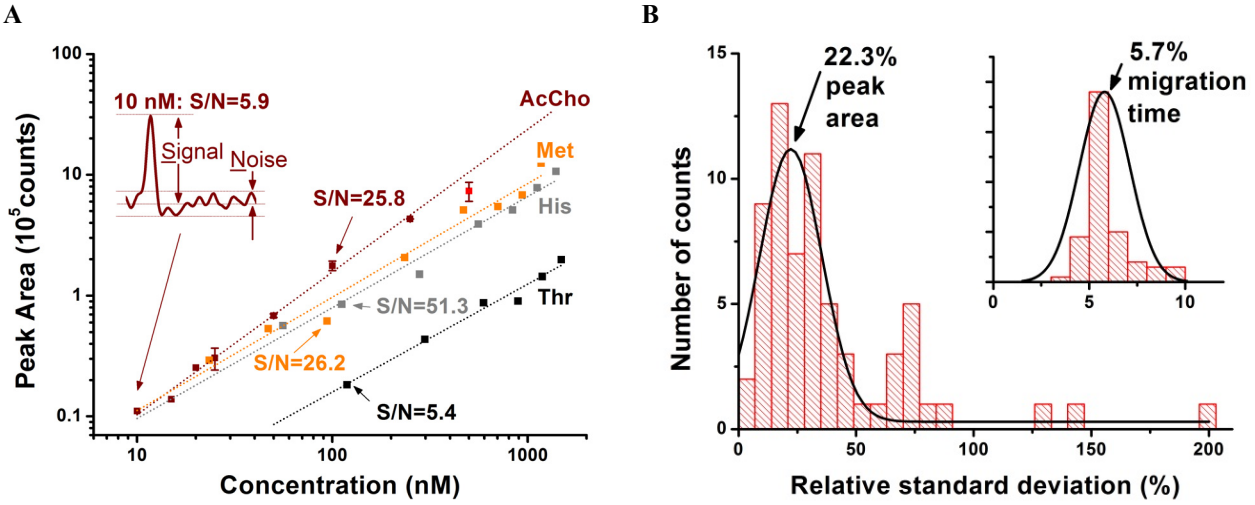

Figure S1. System performance and quantitation for the CE-μESI-MS instrument. **(A)** The lower limit of detection was <10 nM (60 amol) for AcCho with similar performance anticipated for Met (S/N=26.2 at 94 nM) and His (S/N=51.3 at 112 nM) and ~100 nM limit projected for Thr (S/N=5.4 at 119 nM). The inset shows the calculation of signal-to-noise (S/N) ratios for the 10 nM AcCho standard (S/N = 5.9). Calibration curves were linear following the general formula *Peak area (counts)* = *a* + *b* × *c (nM)*, where a/b/regression coefficient (R^2) values are: 2.83/1.18/0.99 for AcCho, 3.06/0.92/0.97 for His, 3.11/0.94/0.97 for Met; and 2.41/0.89/0.98 for Thr. **(B)** Multiple measurement of the $V11_1$ over 4 days demonstrated reproducible performance in quantitation and separation time (inset).

SMALL-MOLECULAR IDENTIFICATIONS

A survey of the mass spectrometric data revealed that ~80 different ion species (molecular features) were detected between all the extracts of the single D11, V11, and V21 blastomeres that were dissected from 16-cell *Xenopus* embryos. Seventy of these features that were used for quantitative analysis are listed in **Table S1**. A subset of these molecular features were identified as small molecules via a multipronged approach that integrated accurate mass measurements, isotope distribution analysis, collision-induced dissociation tandem MS (MS-MS), and comparison of migration times and MS-MS data against chemical standards as well as information available in metabolite tandem MS databases. The combination of multiple orthogonal information to identify a compound upholds high standards that were recently also recommended by international metabolomics societies and initiatives (2-4).

As an example, accurate masses of the molecular features were first searched against metabolite tandem mass spectrometric databases, specifically Metlin (5) and Human Metabolome Database 3.0 (6, 7), with a mass tolerance of 10 ppm, yielding a list of mass (*m/z value)* matches. Next, these mass matches were evaluated by comparing the tandem mass spectrum recorded for the molecular feature with that documented for the putative compound in the databases. **Figure S2** exemplifies the identification of select molecular features. The signal with *m/z* 175.1188 at 18.04 min migration time in the D11 blastomere (top panel) was ascribed to (L/D-)arginine because it matched the mass (*m/z*), electrophoretic migration time, and fragmentation behavior of the L-arginine standard (bottom panel). Likewise, tandem mass spectra are interpreted for signals that were identified as S-adenosylmethionine and serine-arginine. Another example is *m/z* 139.0502, which gave two electropherographic peaks ~2.5 min apart and both signals produced MS/MS

fragmentation patterns that corresponded to cis/trans-urocanic acid on the basis of tandem MS data available in Metlin. The former signal was assigned to the cis isomer based on different times that have been reported under CE conditions (8). In the event that tandem mass data were unavailable in the databases, we further evaluated potential assignments using a chemical standard; the standard related to the positive mass match was measured by our CE-μESI mass spectrometer to determine the migration time and tandem mass spectrum, which were then compared to migration time and fragmentation data collected for the molecular features from the blastomeres. As a result, a total of 40 small molecules were identified with outstanding confidence (**Table S2**), including many amino acids, energy carriers, polyamines, classical neurotransmitters, and even a dipeptide. Note that although differentiation of optical isomers was beyond the goal of this study, CE separations can be extended to chiral dimensions in follow-up experiments. This potential for chiral analysis is illustrated by urocanate, which gave two electropherographic peaks, corresponding to the cis and trans isomers. This careful protocol in identifying metabolites allowed us to monitor small-molecular activity in different blastomeres of the embryo.

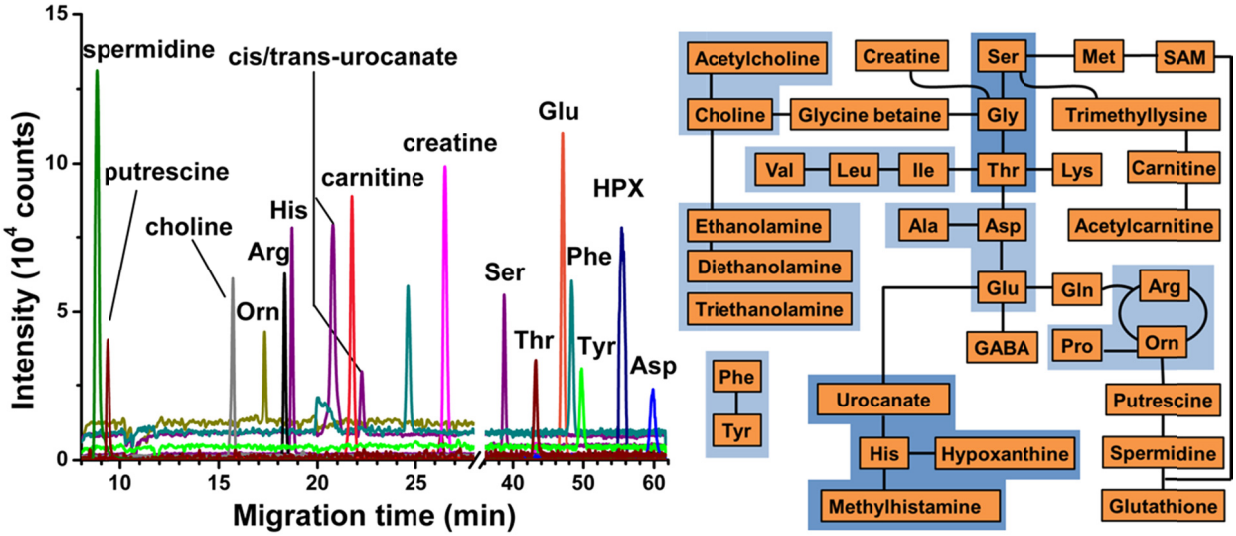

Figure S2. Identification of small metabolites that underpinned central metabolic networks. **(Left)** Representative mass-to-charge (*m/z*)-selected electropherograms for a subset of identified small molecules. Although only a few compounds are shown here, more than 80 different metabolites were detected between all blastomeres in all measurements. **(Right)** Based on the Kyoto Encyclopedia of Genes and Genomes (KEGG) database, 36 different small molecules that were identified in the blastomeres formed metabolic pathways, most connected by common nodes. Darker highlight indicates production at higher abundance. Directions of syntheses and related enzymes are excluded for clarity.

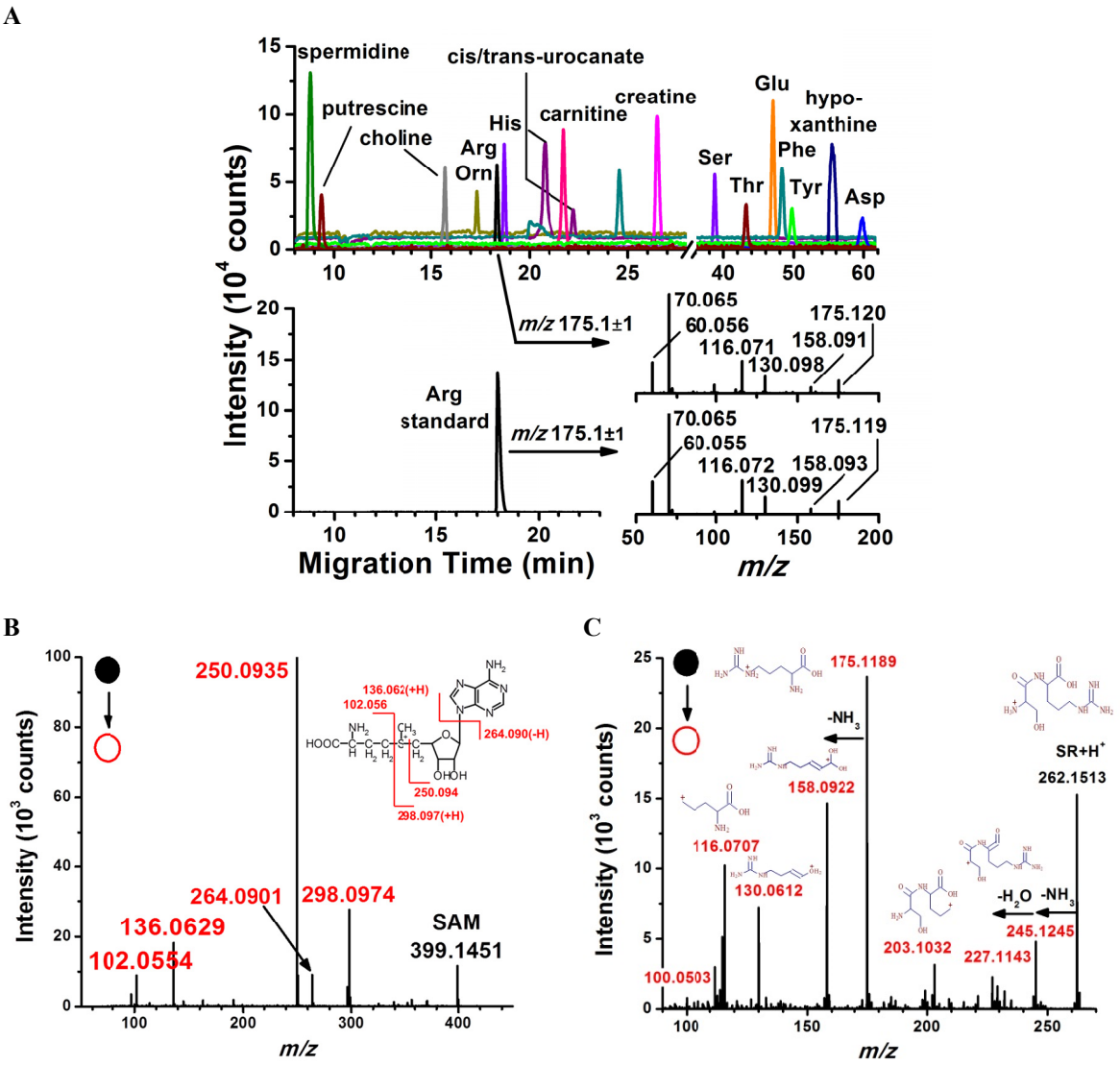

Figure S3. High-confidence small-molecular identifications in single blastomeres. **(A)** Representative mass-to-charge (*m/z*)-selected electropherograms for a subset of identified small molecules. The ion *m/z* 175.1188 at 18.04 min in the D11 blastomere was assigned to arginine by accurate mass measurement, tandem mass spectrometry, and migration time comparison against the standard. Likewise, **(B)** S-adenosylmethionine (SAM) and **(C)** the dipeptide serine-arginine (SR) were identified based on high-resolution tandem mass spectrometry. The detected fragmentation patterns agree with those published at Metlin (accessed on 12/8/2014) and calculated by Mass Frontier 7.0 (Thermo), respectively, providing high-confidence identifications for these small molecules.

METHODS and PROTOCOLS

Chemicals. Acetic acid, formic acid, methanol, and water were from Fisher Scientific (Fair Lawn, NJ). Acetylcholine was from Acros Organics (Fair Lawn, NJ). Eagle's minimum essential medium (Sigma Aldrich; St. Louis, MO) was used as a source of mixture for the following L-amino acid standards: alanine, arginine, asparagine, aspartic acid, glutamic acid, glutamine, glycine, histidine, isoleucine, leucine, lysine, phenylalanine, proline, serine, tyrosine, and valine. All solvents were LC-MS grade, and all chemical standards were reagent grade or higher.

Solutions. Steinberg's solution (100%) was prepared by dissolving the following salts to the indicated concentration using Milli-Q purified water (Millipore): sodium chloride (58.2 mM), potassium chloride (0.67 mM), calcium nitrate (0.34 mM), magnesium sulfate (0.83 mM), trisma hydrochloride (4.19 mM), and trisma base (0.66 mM). The pH of the solution was adjusted to 7.4 using 5 M sodium hydroxide. This solution was diluted two-fold to obtain 50% Steinberg's solution.

Animals (control) and Cell Isolation. Male and female *Xenopus laevis* adult frogs were obtained from Nasco (Fort Atkinson, WI), and maintained in a breeding colony. All protocols related to the maintenance and handling of *Xenopus* were approved by the GW Institutional Animal Care and Use Committee (IACUC no. A311). Fertilized embryos were obtained through gonadotropin-induced natural mating of adult frogs as described elsewhere (9), and their jelly coats were removed following a standard protocol (10). Embryos at the 8-cell stage were transferred into a Petri dish containing 100% Steinberg's solution at room temperature and embryo development was monitored under a stereomicroscope. Upon reaching the 16-cell stage, usually within ~2.75 h post fertilization, the embryos were transferred to 50% Steinberg's solution in an agarose-coated petri dish.

The midline dorsal-animal cell (D11), the midline ventral-animal cell (V11), and the midline ventral-vegetal cell (V21) were identified based on physical appearance (pigmentation) and location in the embryo in reference to established fate maps (11, 12) and dissected from 16-cell frog (*Xenopus laevis*) embryos using a pair of sharpened forceps following a protocol we have described elsewhere (13). For comparison to 32-cell fate maps (14, 15), D11 is the mother blastomere of A1+B1, V11 is the mother blastomere of A4+B4, and V21 is the mother blastomere of C4+D4. A total of n = 5 visually intact blastomeres (biological replicates) were isolated for each cell type, each from different embryos; these were derived from 2 different sets of parents.

Preparation of Ventralized *Xenopus.* For UV light-treated samples, eggs derived from a single female frog were fertilized *in vitro* with sperm from a single male, and the jelly coat removed 10 min after fertilization using standard methods (10). The fertilized clutch was divided into two groups: control siblings and UV-treated. The vegetal poles of the embryos in the latter group were irradiated with UV light at 40 min post-fertilization by standard methods (10), and left unperturbed until reaching the 4-cell stage. Upon reaching the 16-cell stage, blastomeres were dissected and extracted as described below. The remaining UV-treated and control siblings were raised to larval stages and scored for dorsal axial defects according to the Dorsoanterior Index as established elsewhere (16).

We exposed several hundred embryos derived from the same parents to UV-irradiation according to standard protocols (10) and characterized the efficiency of the treatment. In the control,

untreated sibling group, 6.8% of the embryos died by the end of gastrulation (stage 13), and at larval stage 34, 100% (n = 273) were scored as DAI 5, indicating normal development. In UV-irradiated embryos, 4.5% died by the end of gastrulation (stage 13), and at larval stage 34, 10.7% were DAI 5, 10.4% were DAI 3, and 78.9% were DAI 1 and 2, indicating that ~90% had significant dorsoanterior truncations.

Tracking Cell Fates. Metabolite mixtures, one containing 5 mM acetylcholine and 50 mM L-methionine (labelled "m_{V11}") and the other containing 50 mM L-threonine and 50 mM serine (labelled "m_{D11}"), were mixed with either *gfp* mRNA (100 pg/nL) or *nuclear-localized β-galactosidase* (*nβgal*) mRNA (100 pg/nL); the translation of the mRNAs into lineage tracers acts to mark all of the descendants of the blastomere injected with the metabolite mixture throughout development. When embryos reached the 16-cell stage, blastomere V11 on one side of the embryo was injected with 1 nL or 2 nL of the mD11 mixture containing the lineage tracer mRNA. In different embryos, blastomere D11 on one side of the embryo was injected with 1 nL or 2 nL of the mV11 mixture containing the lineage tracer mRNA. Sibling embryos were injected with 1 nL of lineage tracer mRNA only as controls. Embryos injected with *nβgal* mRNA as the lineage tracer were fixed in 4% paraformaldehyde in phosphate buffered saline (PBS) for 1 h, processed for β-gal histochemistry (as previously described in (10)) using magenta-gal (Biosynth International, Inc.) as the chromagen, bleached in a hydrogen peroxide-formamide solution to remove melanin pigment (10) and stored in fixative. Embryos injected with *gfp* mRNA as the lineage tracer were fixed in 4% paraformaldehyde in PBS for 1 h and stored in PBS. For lineage analyses at gastrulation stages (**Fig. S6**), control V11 embryos and m_{D11}-injected V11 (m_{D11}V11) embryos were oriented with the animal pole facing up and imaged at 50×. Using image analysis software (Olympus cellSens software), the midpoint of the animal hemisphere (the animal pole) was calculated and the distance from that point of the furthest cell in the clone was measured. A positive number indicated a position on the dorsal side of the animal hemisphere and a negative number indicated a position on the ventral side. Control D11 embryos and m_{V11}-injected D11 (m_{V11}D11) embryos were oriented with the dorsal side facing up, imaged at 50×, and the width of the clone at its widest point measured. For lineage analyses at larval stages (**Fig. 5**), embryos were examined using epifluorescence optics. The relative contribution to various organs in whole embryo preparations were scored as in the original published fate maps (12) and assigned numbers: "0" indicates no labeled cells in the tissue; "1" indicates fewer than 10 labeled cells; "5" indicates many labeled cells; and "10" indicates that the tissue is comprised almost entirely of labeled cells.

Preparation of Single-blastomere Extracts (Samples). Immediately after isolation, each blastomere was transferred by a sterile glass pipette into a separate microvial (Fisher Scientific; Pittsburgh, PA) containing 100 µL of chilled methanol (~4°C) to denature enzymes and to minimize degradation of small molecules. Afterward, the extracts containing the single blastomeres were dried at 4°C in a vacuum concentrator (Labconco; Kansas City, MO). Last, the content of each vial was reconstituted in 10 µL of 50% (v/v) methanol prepared with 0.5% (v/v) acetic acid, sonicated in ice-cold water for 3 min, and mixed for 1 min using a vortex mixer, allowing us to extract mostly hydrophilic small metabolites from the cells. By altering the composition of this extraction solution, other types of molecules including hydrophobic compounds can be extracted in follow-up studies. Extracts were centrifuged at 8,000×g at 4°C (Sorvall Legend X1R; Thermo Scientific) for 3 min. Blastomere extracts were stored in the extract solutions at –80°C until measurement by CE-µESI-MS. A comparison of signals indicated no detectable change in small-molecular composition in the extracts over the course of

this study (<1 month), as evidenced in **Figure 2**, in which all technical replicates of the same blastomere grouped together during HCA of the CE-MS data (see **Fig. 2**). In agreement, our earlier observation using a similar protocol (17) demonstrated similar success in preserving cell extracts for delayed analysis.

Custom-built CE-μESI-MS System. A single-cell CE-μESI platform was constructed and operated based on our earlier design (18, 19). Briefly, the platform consisted of a stage that accommodated a sample-loading microvial and a background electrolyte (BGE)-containing vial with a capability to vertically translate up to 20 cm in <1 s. The same platform was used to inject the sample and also to separate small molecules. During injection, ~10 nL of the sample was hydrodynamically loaded for 90 s into a 90 cm long fused silica separation capillary with 40/105 μm internal/outer diameter (Polymicro Technologies, Phoenix, AZ) at 15 cm height difference between the capillary outlets.

During separation, the capillary inlet was positioned into the BGE (1% vol/vol formic acid) and electrophoretic separation was performed by applying 19–23 kV to the BGE-containing vial using a regulated high-voltage power supply (model 230-30R; Spellman, Valhalla, NY), which contained the inlet (anode) of the separation capillary. The separation voltage was adjusted to maintain ~7.0–8.5 μA current through the separation capillary. Compounds migrated into a custom-built CE-μESI interface that coaxially supplied 1 μL/min 50% methanol containing 0.1% (vol/vol) acetic acid through a metal emitter (130/260 μm inner/outer diameter) with ends laser-cleaved at right angle. To generate stable electrospray in the cone-jet regime, the emitter was fine-positioned using a three-axis translation stage ~2 mm from the sample plate of the mass spectrometer that was held at –1,700 V using the instrument's control software. As a result, molecules of the blastomeres were separated and efficiently converted to gas-phase ions *in situ*.

Ionized molecules were mass-analyzed between *m/z* 50 and 500 by an orthogonal high resolution time-of-flight mass spectrometer (Impact HD Qq-TOF, Bruker Daltonics, Billerica, MA) operated at a resolving power of 40,000 full width at half maximum (FWHM). External calibration using sodium-formate clusters provided an accuracy of 0.3 mDa across the *m/z* 50–500 range (<0.6 ppm). Molecular identifications were enhanced by data-dependent tandem MS of mass (*m/z*)-selected ions with collision-induced dissociation at ~18 eV in nitrogen gas.

To ensure reproducible system operation without systematic biases in performance, a standard solution containing 50 nM acetylcholine (50% methanol containing 0.5% acetic acid) was measured at the beginning of a series of experiments each day. A reproducibility of <10 relative% error for migration time and <25 relative% error for electropherographic peak area was required before extracts of the blastomeres were measured. In the event that these performance metrics were not met, the system components were thoroughly cleaned and the separation capillary was conditioned using sodium hydroxide as described elsewhere (18). Between consecutive separations, the separation capillary was flushed with BGE for 5 min followed by a 2-min blank run (BGE injected as the analyte) to test the stability of the CE-ESI-MS signal. All experiments reported here were obtained using the same fused silica separation capillary over 1 week of measurements.

Measurement of Blastomere Extracts. Extracts of different cell types were selected and measured in random order the same day according to the following procedure. Samples were allowed to thaw to 4°C in ~3 min, mixed using a vortex-mixer for 1 min, and centrifuged at 10,000×g for 1 min at 4°C (to precipitate cell debris) before measurement. A volume of 1 μL of

each sample was deposited into a clean sample-loading stainless-steel vial, and 10 nL of the sample analyzed by CE-μESI-MS. For quality control, 4 of the n = 5 blastomeres (biological replicates) for each cell type had 2–4 technical replicates that were measured over multiple days. This careful strategy allowed us to test for and to eliminate a potential systematic bias in the measurement of different cell types, the order of their measurement, and the inter-day performance of the instrument. That all technical replicates clustered together during HCA despite their measurement across multiple days indicates that the experiments were devoid of systematic error (see **Fig. 2**).

Data Analysis. Primary (raw) mass spectrometric data files were processed in Compass Data Analysis version 4.0 (Bruker Daltonics) using scripts we have earlier developed (18). Measurement files were externally mass-calibrated using sodium formate clusters that formed in the μESI source as sodium salts were separated from the samples. To find the molecular features in each experiment, selected-ion electropherograms were generated with 500 mDa window with 500 mDa incremental step across the acquisition mass window (*m/z* 50–500), and the resulting time-plots were surveyed for peaks. For each peak, the accurate mass (*m/z* value) was determined by integrating the mass spectrum across the peak. We defined molecular features as ion signals with different accurate masses and different migration times. To determine the abundance of each molecular feature, selected-ion electropherograms were generated for its accurate mass with a 5 mDa selection window, and the peaks were manually integrated. Thus, the resulting metadata was a list of molecular features and corresponding peak areas for 5 biological replicates with 2–4 analytical replicates for the 3 blastomere types for control (untreated) and UV-ventralized *Xenopus* embryos.

Analysis of Statistical and Biological Significance and Multivariate Data Analysis. Statistical analyses were performed using two-tailed t-tests performed with $P < 0.05$ threshold indicating statistical significance with blastomeres of identical type irrespective of parental origin serving as one group. A fold change of at least 2.0 was considered biologically significant. The metadata were further evaluated in MetaboAnalyst 2.0 (20), a public web-based metabolomic pipeline. Euclidean method was selected to calculate the distance matrix and Ward method was used to generate data clusters. Statistical and biological significance thresholds were $P < 0.05$ (t-test) and fold change of higher than 2.0. Molecular feature selection was limited to the signals that had the highest statistical significance. The number of features selected is identified in the figure captions.

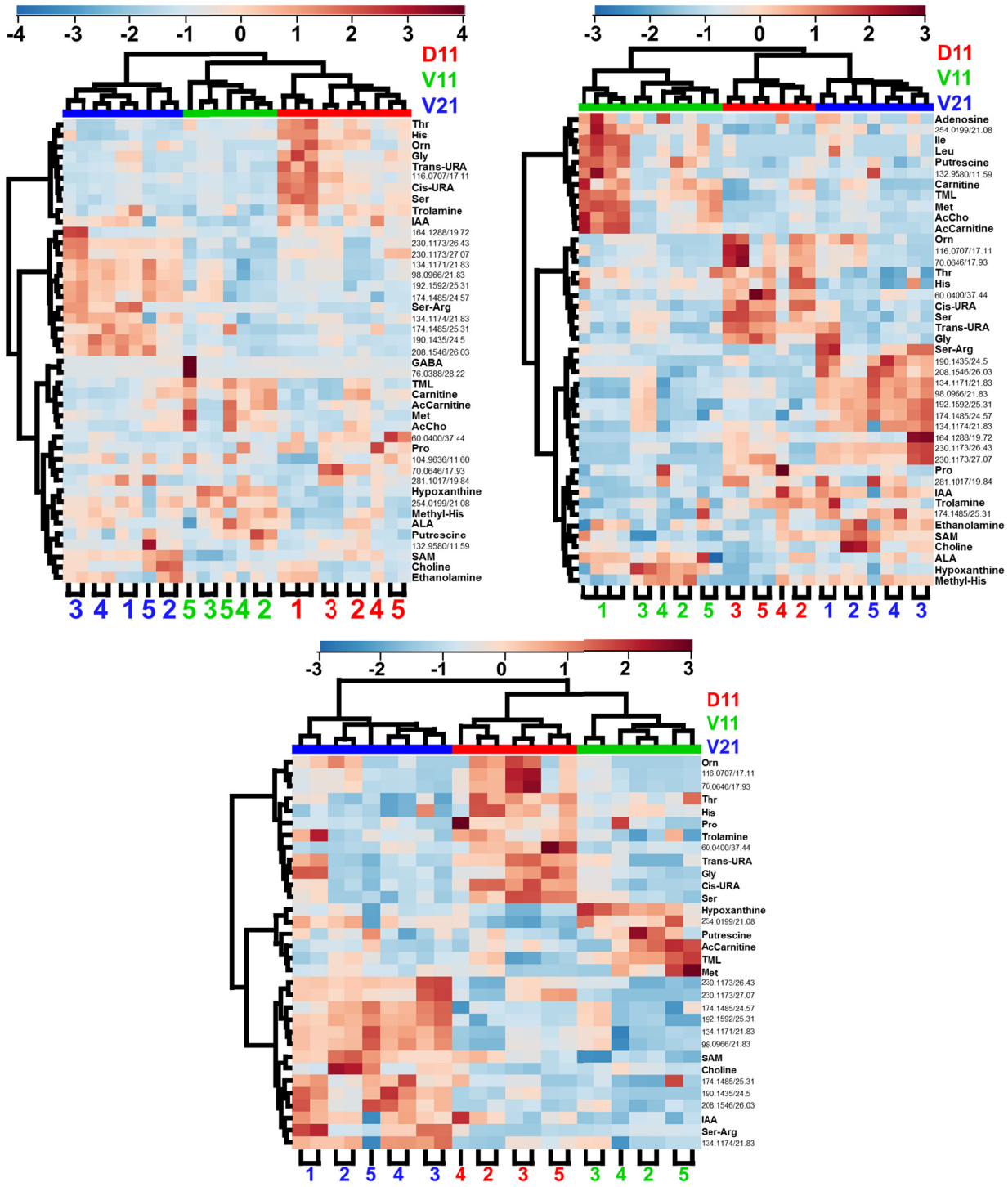

Figure S4. Confirmatory analysis of blastomere type-specific metabolic composition. Elimination of the **(Top left)** $V11_1$, **(Top right)** $D11_1$, or **(Bottom)** both of these blastomeres leaves the clustering of other blastomeres based on metabolic composition unaffected. Top statistically most significant features are shown. Yet unidentified small molecular features are listed as accurate mass/migration time (min) data.

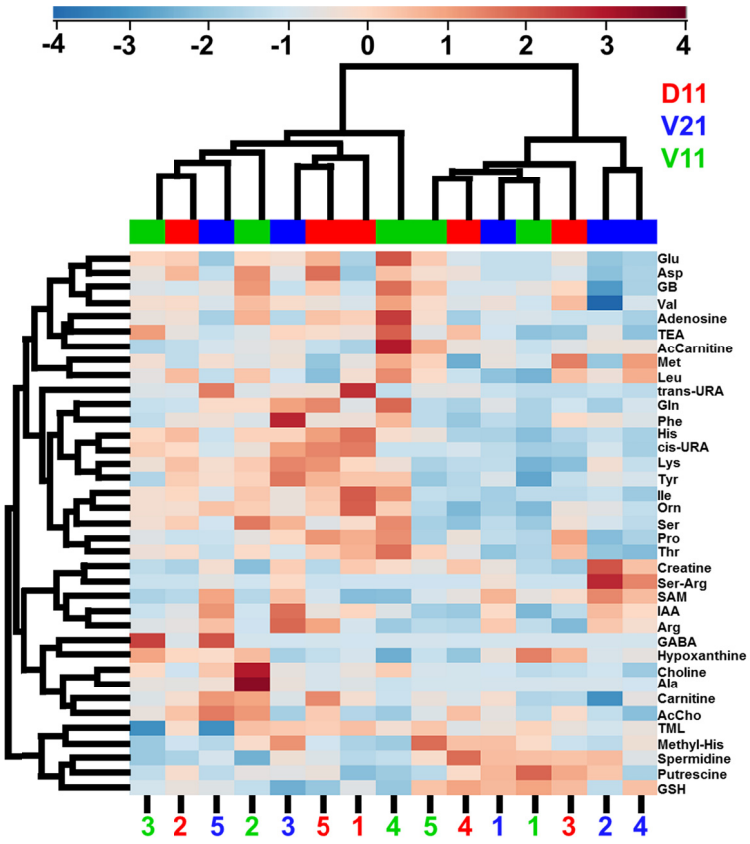

Figure S5. Hierarchical cluster analysis and heat map for D11, V11, and V21 blastomeres from ventralized embryos. Upon UV-ventralization, small-molecular cell heterogeneity that was characteristic for the untreated (control) embryos was lost (beyond detection limits), indicating that metabolic differences between the D11, V11, and V21 blastomeres are caused by cell type rather than the size, pigmentation, or location of the cell in the embryo.

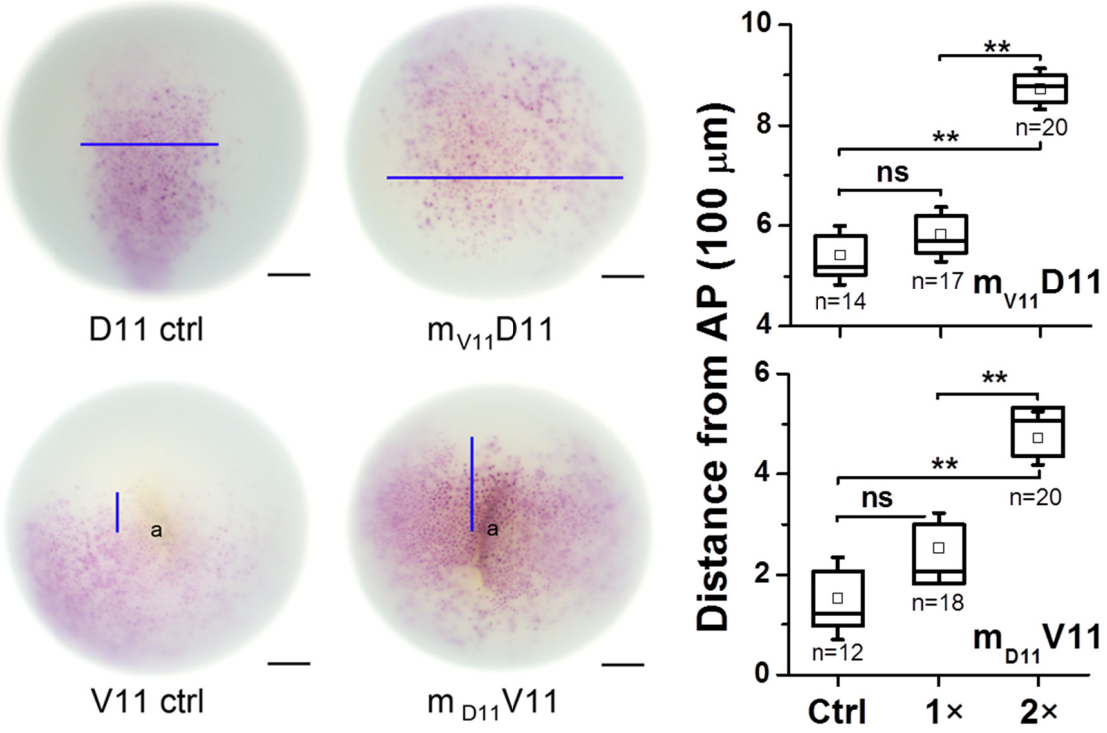

Figure S6. Gastrula stages injected with *nβgal* mRNA alone (D11 ctrl; V11 ctrl) or metabolites plus *nβgal* mRNA (m_{V11}D11; m_{D11}V11). Pink cells are descended from the injected blastomere. **(Top row)** In dorsal views of D11 ctrl embryos, the descendants are closely packed along the midline as the result of convergent-extension movements during gastrulation. In m_{V11}D11embryos, the descendants are scattered across the dorsal surface. Measurements of the width of the clone (blue bars in D) are significantly different between control and metabolite-injected embryos. **(Bottom row)** In animal hemisphere views of V11 ctrl embryos, the descendants are mostly in the ventral half (bottom) of the embryo; a few cells are located in the dorsal half (top). In m_{D11}V11 embryos, the descendants are scattered across the animal hemisphere; a large number of cells are located in the dorsal half. Measuring the distance between the furthest cells in the clone from the animal pole (a) (blue bars) shows significant differences between control and metabolite-injected embryos. Scale bars = 180 μm for all images. Statistical significance is marked at **P* < 0.05 and ***P* < 0.005. Key to box-whisker plots: square = mean; box = 1 × SE; whisker = 1.5 × SE.

Table S1. Molecular features (accurate mass *vs.* migration time in min) monitored among single blastomeres of 16-cell *Xenopus* embryos. Although more than 80 different features were detected between the cells, 70 are listed here that were used for quantitative analysis. Fields in bold mark ions that were identified in the study (**Table S2**). Fields in grey highlight features that were utilized for multivariate and statistical analysis.

361.8096 (7.98)	**146.1648 (8.70)**	72.0801 (9.27)	140.9523 (11.39)	132.958 (11.62)
104.9636 (11.67)	132.958 (12.23)	104.9636 (12.25)	62.0594 (13.02)	**62.0600 (13.98)**
184.1442 (14.24)	**104.1068 (15.53)**	86.0958 (15.96)	**262.1507 (16.67)**	**399.1445 (16.78)**
106.0861 (38.34)	116.0707 (17.04)	**147.1129 (17.25)**	70.0646 (17.96)	**175.1188 (18.04)**
281.1017 (18.19)	**189.1597 (18.32)**	**156.0768 (18.45)**	**146.1182 (19.60)**	164.1288 (19.73)
134.1174 (19.93)	**139.0502 (20.61)**	156.0875 (21.00)	254.0199 (21.12)	**162.1124 (21.52)**
134.1171 (21.84)	121.0393 (21.94)	**139.0502 (22.06)**	190.1435 (22.23)	174.1485 (22.29)
98.0966 (23.48)	146.1539 (23.82)	**204.123 (24.04)**	192.1592 (25.42)	**76.0388 (25.68)**
132.0767 (25.95)	**90.0549 (25.97)**	208.1546 (26.29)	230.1173 (26.69)	230.1173 (27.38)
76.0388 (27.50)	239.1063 (28.00)	**118.087 (36.54)**	86.0960 (37.27)	60.0436 (37.81)
106.0498 (37.84)	86.096 (38.13)	190.0025 (38.75)	**120.0653 (42.19)**	56.0490 (42.57)
188.0708 (42.76)	**147.0773 (44.45)**	102.9703 (45.63)	**148.0606 (46.02)**	**166.0865 (47.23)**
182.0813 (48.56)	70.0648 (50.45)	**116.0708 (50.54)**	**137.0457 (54.62)**	74.0231 (58.45)
134.045 (58.53)	**118.087 (59.75)**	74.0231 (61.85)	157.0838 (68.40)	**308.0917 (68.65)**

Table S2. Small molecules identified from single blastomeres of the 16-cell *Xenopus* embryo.

ID	Compound (Abbrev.)		Formula†	t_m (min)	*m/z* measured	*m/z* theor.‡	Δ (mDa)	Δ (ppm)
1	Spermidine**		$C_7H_{19}N_3$	8.70	146.1648	146.1652	0.4	2.7
2	Putrescine		$C_4H_{12}N_2$	8.70	89.1071	89.1073	0.2	2.2
3	Methylhistamine		$C_6H_{11}N_3$	9.42	126.1022	126.1026	0.4	3.2
4	Ethanolamine		C_2H_7NO	13.98	62.0600	62.0600	0.0	0.0
5	Choline*,**	Cho	$C_5H_{13}NO$ (+)	15.53	104.1068	104.1070	0.2	1.9
6	Ser-Arg**	SR	$C_9H_{19}N_5O_4$	16.67	262.1507	262.1510	0.3	1.1
7	S-adenosyl-methionine**	SAM	$C_{15}H_{22}N_6O_5S$	16.78	399.1445	399.1445	0.0	0.0
8	Ornithine**	Orn	$C_5H_{12}N_2O_2$	16.90	133.0984	133.0972	-1.2	-9.0
9	Lysine*,**	Lys	$C_6H_{14}N_2O_2$	17.25	147.1129	147.1128	-0.1	-0.7
10	Arginine*,**	Arg	$C_6H_{14}N_4O_2$	18.04	175.1188	175.1190	0.2	1.1
11	y-aminobutyric acid	GABA	$C_4H_9NO_2$	18.22	104.0711	104.0706	-0.5	-4.8
12	N6,N6,N6-trimethyl-lysine	TML	$C_9H_{20}N_2O_2$	18.32	189.1597	189.1598	0.1	0.5
13	Histidine*,**	His	$C_6H_9N_3O_2$	18.45	156.0768	156.0768	0.0	0.0
14	Acetylcholine*,**	AcCho	$C_7H_{15}NO_2$ (+)	19.60	146.1182	146.1176	-0.6	-4.1
15	Trolamine	TEA	$C_6H_{15}NO_3$	20.51	150.1125	150.1125	0.0	0.0
16	Cis-urocanate**	cURA	$C_6H_6N_2O_2$	20.61	139.0502	139.0502	0.0	0.0
17	Carnitine*,**	Car	$C_7H_{15}NO_3$	21.52	162.1124	162.1125	0.1	0.6
18	Trans-urocanate**	tURA	$C_6H_6N_2O_2$	22.06	139.0502	139.0502	0.0	0.0
19	Acetylcarnitine*,**	AcCar	$C_9H_{17}NO_4$	24.04	204.1230	204.1230	0.0	0.0
20	Glycine*	Gly	$C_2H_5NO_2$	25.68	76.0388	76.0393	0.5	6.6
21	Creatine*,**	CR	$C_4H_9N_3O_2$	25.95	132.0767	132.0768	0.1	0.8
22	Alanine*	Ala	$C_3H_7NO_2$	25.97	90.0549	90.0550	0.1	1.1
23	Adenosine**		$C_{10}H_{13}N_5O_4$	27.56	268.1042	268.1040	-0.2	-0.8
24	Valine*,**	Val	$C_5H_{11}NO_2$	36.54	118.0870	118.0863	-0.7	-5.9
25	Isoleucine*	Ile	$C_6H_{13}NO_2$	37.26	132.1024	132.1019	-0.5	-3.8
26	Serine*,**	Ser	$C_3H_7NO_3$	37.84	106.0498	106.0499	0.1	0.9
27	Leucine*	Leu	$C_6H_{13}NO_2$	37.90	132.1025	132.1019	0.6	0.7
28	Diethanolamine		$C_4H_{11}NO_2$	38.34	106.0861	106.0863	0.2	1.9
29	Threonine*,**	Thr	$C_4H_9NO_3$	42.19	120.0653	120.0655	0.2	1.7
30	Indoleacrylate*	IAA	$C_{11}H_9NO_2$	42.76	188.0708	188.0706	-0.2	-1.1
31	Methionine*	Met	$C_5H_{11}NO_2S$	44.40	150.0589	150.0583	-0.6	-4.0
32	Glutamine*,**	Gln	$C_5H_{10}N_2O_3$	44.45	147.0773	147.0764	-0.9	-6.1

ID	Compound (Abbrev.)		Formula†	t_m (min)	*m/z* measured	*m/z* theor.‡	Δ (mDa)	Δ (ppm)
33	Glutamate*,**	Glu	$C_5H_9NO_4$	46.02	148.0606	148.0604	-0.2	-1.4
34	Phenylalanine*,**	Phe	$C_9H_{11}NO_2$	47.23	166.0865	166.0863	-0.2	-1.2
35	Tyrosine*,**	Tyr	$C_9H_{11}NO_3$	48.56	182.0813	182.0812	-0.1	-0.5
36	Proline*,**	Pro	$C_5H_9NO_2$	50.54	116.0708	116.0706	-0.2	-1.7
37	Hypoxanthine**	HPX	$C_5H_4N_4O$	54.62	137.0457	137.0458	0.1	0.7
38	Aspartate*,**	Asp	$C_4H_7NO_4$	58.53	134.0450	134.0448	-0.2	-1.5
39	Glycine betaine*	GB	$C_5H_{11}NO_2$	59.75	118.0870	118.0863	-0.7	-5.9
40	Glutathione*	GSH	$C_{10}H_{17}N_3O_6S$	68.65	308.0917	308.0911	-0.6	-1.9

Note: In addition to an agreement in accurate mass, asterisk (*) indicates identifications that are also based on migration time comparison to chemical standards, and two asterisks (**) mark identifications that were further supplemented by MS/MS using chemical standards and/or comparison of measured MS/MS data to those available at Metlin. †Compounds were detected as singly protonated quasimolecular ions unless specified. ‡Theoretical *m/z* values were calculated using IsotopePattern version 2.0 (Bruker Daltonics).

Table S3. Relative metabolite abundances between single blastomeres in the untreated (control) and ultraviolet (UV)-ventralized embryos.

Compound		Control									UV-ventralized								
		D11/V11			V11/V21			D11/V21			D11/V11			V11/V21			D11/V21		
ID	Name	Ratio	p value		Ratio	p value		Ratio	p value		Ratio	p value		Ratio	p value		Ratio	p value	
19	AcCar	-2.2	0.04607	*	2.2	0.05441		-1.0	0.98931		-1.1	0.83691		-1.3	0.31433		-1.4	0.10585	
14	AcCho	-2.1	0.02339	*	1.8	0.08326		-1.2	0.39543		1.3	0.23231		-1.6	0.03137	*	-1.2	0.25593	
6	Ser-Arg	-3.6	0.00125	**	-3.9	0.00359	**	-13.7	0.00094	**	-1.2	0.69437		-8.9	0.00564	**	-10.5	0.00114	**
5	Choline	1.3	0.38654		-2.5	0.02115	*	-1.9	0.10516		-1.4	0.15097		-1.2	0.44031		-1.7	0.02190	*
16	cURA	6.9	0.00069	**	-1.5	0.24240		4.5	0.00482	**	-1.0	0.94946		1.2	0.76063		1.2	0.54103	
39	GB	2.9	0.05018	*	-4.3	0.00035	**	-1.5	0.16949		1.0	0.94328		-1.2	0.17444		-1.2	0.19498	
20	Gly	7.0	0.00147	**	-3.1	0.08122		2.3	0.07972		1.0	1.00000		1.0	1.00000		1.0	1.00000	
37	HPX	-3.0	0.00236	**	1.1	0.62779		-2.7	0.00065	**	-1.6	0.04240	*	1.0	0.97489		-1.6	0.00676	**
30	IAA	1.7	0.00189	**	-2.2	0.00013	**	-1.3	0.12443		1.2	0.26093		-2.6	0.00003	**	-2.1	0.00002	**
31	Met	-2.2	0.02027	*	1.5	0.17712		-1.5	0.02176	*	-1.1	0.57954		-1.5	0.02156	*	-1.6	0.00554	**
8	Orn	10.0	0.00191	**	-4.3	0.03869	*	2.3	0.08655		1.3	0.33955		-1.4	0.22425		-1.1	0.64912	
34	Phe	2.5	0.00049	**	-1.8	0.00649	**	1.3	0.15937		-1.0	0.84814		-1.6	0.00725	**	-1.6	0.00107	**
36	Pro	3.0	0.00447	**	-1.8	0.00890	**	1.6	0.11840		1.1	0.72480		-1.1	0.70654		-1.0	0.99173	
7	SAM	1.8	0.05345		-3.0	0.00093	**	-1.7	0.01404	*	2.0	0.04465	*	-4.7	0.00001	**	-2.4	0.00028	**
26	Ser	5.7	0.00062	**	-1.2	0.52156		4.6	0.00365	**	-1.1	0.62892		-1.4	0.10751		-1.6	0.00686	**
15	TEA	4.4	0.00007	**	-3.4	0.02731	*	1.3	0.37251		1.2	0.67874		1.2	0.56844		1.4	0.30437	
29	Thr	3.6	0.00728	**	1.1	0.81380		4.0	0.01407	*	-1.0	0.78216		-1.1	0.43465		-1.2	0.23879	
18	tURA	7.9	0.00098	**	-2.6	0.08627		3.0	0.02299	*	1.5	0.54927		-1.5	0.49649		-1.1	0.92809	
35	Tyr	4.7	0.00013	**	-3.5	0.00021	**	1.3	0.21167		1.1	0.53496		-1.7	0.00248	**	-1.6	0.00145	**

Note: Statistical significance is marked at *P < 0.05 and **P < 0.005.

Table S4. Quantitation of select metabolites that were differentially produced between D11 and V11 blastomeres for an average 90-nL-volume blastomere in the 16-cell embryo.

Metabolite	pmol/blastomere				
	$D11_6$	$D11_7$	$D11_8$	Average	RSD
His	15.1	9.1	5.5	**9.9**	**4.9**
Thr	17.6	10.5	6.2	**11.5**	**5.8**
	$V11_6$	$V11_7$	$V11_8$	Average	RSD
AcCho	1.3	0.9	12.	**1.2**	**0.2**
Met	21.7	10.2	38.5	**23.5**	**14.2**
Ala	n/d	25.8	39.8	**32.8**	**9.9**

Note: n/d, not detected. RSD indicates relative standard deviation.

REFERENCES

1. Vastag L, *et al.* (2011) Remodeling of the metabolome during early frog development. *PLoS One* 6(2):e16881.
2. Creek DJ, *et al.* (2014) Metabolite identification: are you sure? And how do your peers gauge your confidence? *Metabolomics* 10(3):350-353.
3. Sumner LW, *et al.* (2007) Proposed minimum reporting standards for chemical analysis. *Metabolomics* 3(3):211-221.
4. Schymanski EL, *et al.* (2014) Identifying Small Molecules via High Resolution Mass Spectrometry: Communicating Confidence. *Environ. Sci. Technol.* 48(4):2097-2098.
5. Zhu ZJ, *et al.* (2013) Liquid chromatography quadrupole time-of-flight mass spectrometry characterization of metabolites guided by the METLIN database. *Nat. Protoc.* 8(3):451-460.
6. Wishart DS, *et al.* (2009) HMDB: a knowledgebase for the human metabolome. *Nucleic Acids Res.* 37:D603-D610.
7. Wishart DS, *et al.* (2013) HMDB 3.0-The Human Metabolome Database in 2013. *Nucleic Acids Res.* 41(D1):D801-D807.
8. Hermann K & Abeck D (2000) Determination of histidine and urocanic acid isomers in the human skin by high-performance capillary electrophoresis. *J. Chromatogr. B* 749(1):41-47.
9. Moody S (2000) Cell Lineage Analysis in Xenopus Embryos. *Developmental Biology Protocols,* Methods in Molecular Biology™, eds Walker J, Tuan R, & Lo C (Humana Press), Vol 135, pp 331-347.
10. Sive HL, Grainger RM, & Harland RM (2000) *Early development of Xenopus laevis: A laboratory manual* (Cold Spring Harbor Laboratory Press {a} , 10 Skyline Drive, Plainview, NY, 11803-2500, USA) p i.
11. Hirose G & Jacobson M (1979) Clonal organization of the central nervous system of the frog: 1. Clones stemming from individual blastomeres of the 16-cell and earlier stages. . *Dev. Biol.* 71(2):191-202.
12. Moody SA (1987) Fates of the blastomeres of the 16-cell stage Xenopus embryo. *Dev. Biol.* 119(2):560-578.

13. Grant PA, Herold MB, & Moody SA (2013) Blastomere explants to test for cell fate commitment during embryonic development. *Journal of visualized experiments : JoVE* (71).
14. Nakamura O, Takasaki H, & Nagata A (1978) Further studies of the prospective fates of blastomeres at the 32-cell stage of Xenopus laevis embryos. *Medical Biology* 56(6):355-360.
15. Dale L & Slack JMW (1987) Fate map for the 32-cell stage of Xenopus laevis. *Development* 99(4):527-551.
16. Kao KR & Elinson RP (1988) The entire mesodermal mantle behaves as Spemann organizer in dorsoanterior enhanced Xenopus laevis embryos. *Dev. Biol.* 127(1):64-77.
17. Nemes P, Knolhoff AM, Rubakhin SS, & Sweedler JV (2011) Metabolic differentiation of neuronal phenotypes by single-cell capillary electrophoresis electrospray ionization mass spectrometry. *Anal. Chem.* 83(17):6810-6817.
18. Nemes P, Rubakhin SS, Aerts JT, & Sweedler JV (2013) Qualitative and quantitative metabolomic investigation of single neurons by capillary electrophoresis electrospray ionization mass spectrometry. *Nat. Protoc.* 8(4):783-799.
19. Lapainis T, Rubakhin SS, & Sweedler JV (2009) Capillary electrophoresis with electrospray ionization mass spectrometric detection for single-cell metabolomics. *Anal. Chem.* 81(14):5858-5864.
20. Xia JG, Mandal R, Sinelnikov IV, Broadhurst D, & Wishart DS (2012) MetaboAnalyst 2.0-a comprehensive server for metabolomic data analysis. *Nucleic Acids Res.* 40(W1):W127-W133.